

## Study on the Influence of Fluid Parameters on Transverse Vibrations of Polytetrafluoroethylene Bellows Expansion Joint

Sujan Rao. Nakkanti<sup>1</sup>, Radhakrishna. M<sup>2</sup>, A.M.K. Prasad<sup>3</sup>

<sup>1</sup>(Mechanical Engineering Department, Sai Spurthi Institute of Technology, Sathupally, Telangana, India,

<sup>2</sup>(Design and Engineering, CSIR-Indian Institute of Chemical Technology, Tarnaka, Hyderabad, India

<sup>3</sup>(Department of Mechanical Engineering, University College of Engineering, OU, Hyderabad, India

Corresponding Author: Sujan Rao. Nakkanti

**Abstract :** - This work deals with the fluid conveying fixed-fixed end conditions of U-shaped Polytetrafluoroethylene bellows expansion joint. A mathematical equation is modeled for calculating the transverse natural frequencies. It is assumed that the mass distribution of bellows is uniform and considered for influence of different inlet pressures and velocities on the transverse vibrations of various modes of frequencies of bellows which convey liquids (water). The equation was derived using the Timoshenko elastic beam theory for fixed-fixed beam conditions. Further the non-homogeneous transcendental equation is solved using the Bisection method in FORTRAN compiler to predict the stability and transverse vibrations. The diameter of 3" U-shaped bellows specimens were chosen to perform experimental investigations for different input pressures and velocities measured by suitable pressure gauges and rotameter respectively. The derived equations of pressure and velocity inputs are analyzed for critical values. The resulting experimental data have proven that the deduced equation predictions are accurate enough to meet standard engineering requirements.

**Keywords:** -bellows, critical velocity, natural frequency, Polytetrafluoroethylene, transverse vibration.

Date of Submission: 07-06-2018

Date of acceptance: 23-06-2018

### I. INTRODUCTION

In recent times, non-metallic bellows expansion joint has been found to be more compatible with many potential industrial applications, particularly in fluid conveying piping systems. This is because of its good mechanical, chemical and thermal properties at par with any metallic expansion joint. Several types of continuum-based elasticity theories were modeled as an elastic corrugated cylindrical tube representing a bellows expansion joint, and the mechanics and dynamic response of bellows expansion joint were studied. The bellows expansion joints are thin-walled corrugated tubes designed for high flexibility when subjected to longitudinal loads, internal pressure or bending moments. Theoretical and experimental studies on bellows published since the first analysis in 1932 are reviewed herein. A bellows, or a closed thin-walled elastic tube with corrugated walls, undergoes longitudinal extension when subjected to internal fluid pressure and inlet velocity.

Jakubauskas V. F et al.[1] presents the results of a natural frequencies of fluid-added mass of fluid-filled bellows expansion joints. The bellows were modeled using axisymmetric finite elements, while the fluid region was discretized using axisymmetric triangular elements. Based on boundary conditions, the potential flow model for the fluid and the added mass determined for each bellows mode. This added mass was then used to determine the in-fluid bellows natural frequencies. Experiments were conducted to verify the theoretical model and agreement was found to be very good. Jakubauskas V. F et al. [2] considered the transverse vibrations of fluid-filled double-bellows expansion joints. The bellows are modeled as a Timoshenko beam, the fluid added mass includes rotary inertia and bellows convolution distortion effects. The natural frequencies are also given in terms of Rayleigh quotient for both lateral and rocking modes of the pipe connecting the bellows. The theoretical predictions for the modes are compared with experiments in air and water and the agreement is found to be very good. The Strouhal numbers are computed for each of the flow-excited mode resonances. Jakubauskas V. F et al.[3] presented the results shows under the influence of the fluid-added mass in bellows expansion joints during bending vibrations, one due to transverse rigid-body motion and the other due to distortion of the convolutions during bending. The distortion component was determined using finite element analysis, and the results are presented in a graphical form for a typical range of bellows geometries. Jakubauskas V. F et al[4] developed a theoretical model based on Timoshenko beam theory for the transverse vibrations of bellows expansion joints. The author developed in the form of a Rayleigh quotient and is presented in a way for hand calculations for bellows natural frequencies. The results for the fundamental modes transverse modes are

compared with experiments as well as the predictions of the simplified analysis of the Expansion Joint Manufacturers Association (EJMA). While the present analysis agrees well with experiments, the EJMA approach can be substantially in error due to neglect the effect of rotary inertia and the convolution distortion component. Jakubauskas V. F et al[5] presented the results of investigation of the fluid added mass in axial vibrations of bellows expansion joints. The added mass is shown to consist of three parts, one due to convolution translation in axial direction, due to distortion of the convolution during vibration and the due to the return flow in central section of bellows. The distortion component for a half-convolution has been determined using finite element analysis and the results are presented in graphical form for a typical range of bellows geometry. The total added mass is given in a form suitable for hand calculations.

Radhakrishna M et al. [6] presented paper aims at finding out the effect of elastically restrained ends on the axial natural frequencies. The analysis considers finite stiffness axial restraints on the bellows, i.e. solving the set of equations with non-homogeneous boundary conditions. Two bellow specimens are considered for comparison having the same dimensions. The transcendental frequency equation deduced is accurate as the first, second and third mode frequencies computed are in close agreement to the ones obtained. Watanabe M et al. [7] dealt with the theoretical stability analysis and experimental study of flexible bellows at fixed at both ends rigidly subjected to periodic internal fluid pressure excitation. The basic equation of the bellows derived as a Mathieu's equation subjected to periodic internal fluid pressure excitation. Natural frequencies of the bellows are examined and stability maps are presented for parametric instability, computed by Bolotin's method. Author presented that the buckling occurs due to high internal fluid pressure and transverse natural frequencies of the bellows decrease with increasing the static internal fluid pressure. Parametric instability regions are clarified and the theoretical and experimental are evaluated and parametric instability regions are clarified. Faraji .G et.al. [8]proposed for manufacturing of the metal bellows based on the influencing parameters such as initial length of tube, internal pressure, axial feeding and velocity, mechanical properties and the type of materials were investigated using finite element (FE) analysis (LS-Dyna) and experimental tests. The results of the work used as a basis of designing a new type of the metal bellows. Price DM et al.[9]using an instrumented thermal conductivity apparatus (Lees' disk) and by DSC the thermal conductivity of Polytetrafluoroethylene (PTFE) was studied. The effect of crystallinity on thermal conductivity was investigated and compared with different methods. The incorporation of metal (Aluminum) flakes raised heat transport through the composites and thermal conductivity of PTFE with different levels of crystallinity was measured at 232°C and shown to increase linearly with this parameter. Rae PJ et al.[10] were tested Samples of DuPont 7A and 7C Teflon, PTFE in compression at strain-rates between 10<sup>-4</sup> and 1 s<sup>-1</sup> and temperatures between -198 and 200°C. The strain gauges were used to measure and quantified axial and transverse strain. The affected of strain-rate and temperature on mechanical properties were found. Several techniques were adapted for finding physical properties of the sintered PTFE. Wilson JF[11] summarized the key results dealt with load-deflection behavior. Non- dimensional material parameters and corrugation geometries were used for results, comparison and evolution. In experimental results the classical beam, plate, and shell theories were used for mechanical behavior of polyethylene bellows. Wilson JF[12] Investigated the mechanical behavior of several pressurized bellows, which are subjected to compression longitudinally, designed to bend and twist. Bellows in clusters in a cylindrical helix whose angle is chosen to predict mechanical (load-displacement relationships for given bending and torsional input) behavior and compared with experimental results. Becht C[13]suggested and predicted the fatigue behavior of the bellows expansion joint based on the combination of analysis because one of the reasons for the unreliability is plastic strain concentration in number of convolutions. The author predicted and compared that the difference of strain concentration between reinforced and unreinforced bellows and better predicted by fatigue life of the bellows fatigue data based on a geometry parameter. Tingxin L et al.[14]presented experimental results and analysis of toroidal bellows behavior compared with U-shaped bellows. Based on the analysis toroidal bellows expansion joint have exhibited better results and is more suited for higher internal pressure situations due to smaller internal pressure-induced stress, longer fatigue life, stronger ability to resist internal pressure instability. Shaikh H et al.[15]presented the failure of an AM 350 steel bellows, which are used in the control mechanism of the fast breeder test reactor (FBTR). The leak test was carried due to visual inspection of the leak area did not indicate defects. A few of pits had propagated through the thickness of bellows and corrosion products revealed the presence of chlorides. Suspected to have caused the pitting in marine atmosphere during a storage period of 13 years was found. Nishiguchi. I et al.[16]investigated in plane squirm of rectangular bellows and proposed a simplified evaluation technique based on the half pitch model and compared with that of circular bellows. The elastic squirm is governing with a relatively high length-to-diameter ratio for the bellows with a lower number of convolutions. Broman.G.I[17]presented the analysis to determine dynamic characteristics of in finite elements of I-DEAS Master Series 6. This is advantageous that system to be optimized with respect to design parameters. Stress in the bellows can be predicted by this known dynamic behavior. This method has the potential of considering axial, bending and torsion degrees of freedom simultaneously, also modeled by beam or shell finite elements. Li T.X et al. [18] deduced the equations for

calculating the longitudinal and transverse natural frequencies of U-shaped bellows with different end conditions, on the basis of mass distribution of bellows is uniform. Author also discussed the influence of different axial extension and compression on the natural frequencies of bellows which either contain gas or are filled with liquids. Eleven U-shaped bellows specimens were chosen to perform experiments, applying the 'shock' method and the 'resonance' method respectively. The resulting experimental data have proven that the deduced equations are accurate enough to meet standard engineering requirements.

## II. MATHEMATICAL MODEL AND ANALYSIS

A schematic diagram of a PTFE bellows expansion joint embedded in elastic medium with the two ends fixed for conveying fluid, is considered as a hollow corrugated tube as shown in Fig. 1. The transverse displacement 'w' of the PTFE bellows expansion joint is dependent on time- 't' and the spatial coordinate-'s'.

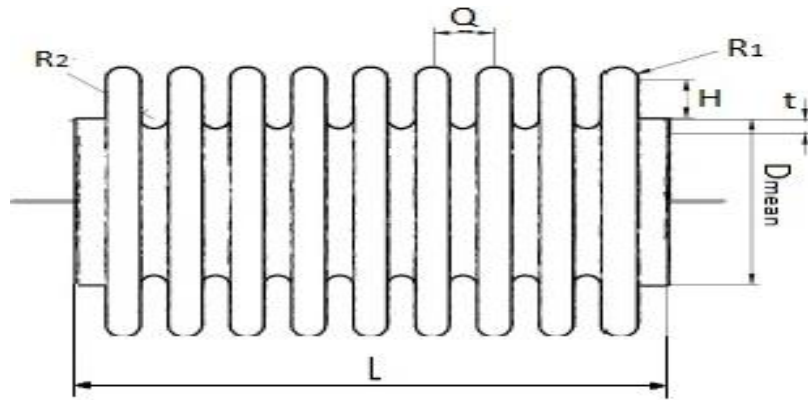


Figure.1. Geometry of bellows expansion joint

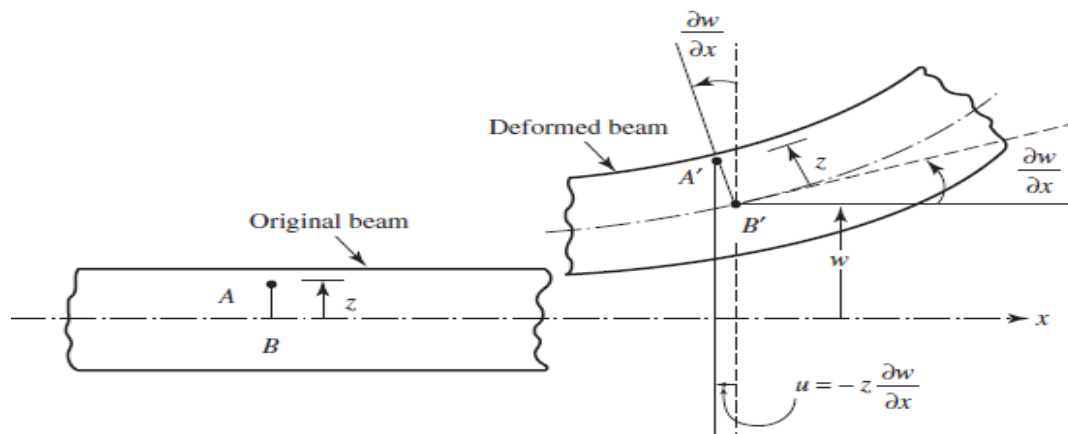


Figure.2. Bending of the beam element

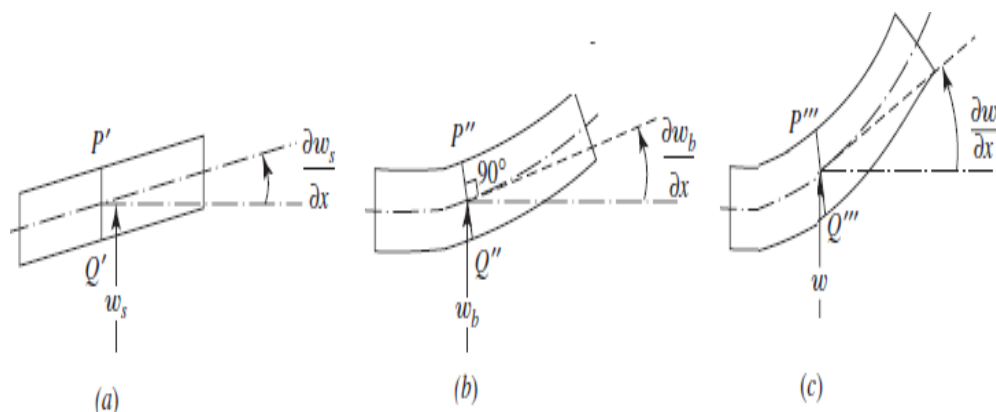


Figure.3. Beam elements with (a) shear, (b) bending and (c) total deformation

Here  $\beta i = \frac{\partial w}{\partial x}$  is shear deformation or shear angle in Fig. (3)(a). The fibers are located in an element at distance at a 'z' from the centerline. The shear deformation has no effect to cause any axial displacement. Hence, the components of displacement can be expressed as

$$u = -z \left( \frac{\partial w}{\partial x} - \beta i \right) = -z \phi(x, t), v = 0 \text{ and } w = w(x, t) \quad (1)$$

The PTFE bellows expansion joint has an equivalent bending rigidity EI and length L with the crown and root radii of R<sub>1</sub> and R<sub>2</sub> and a thickness, t [3-5]. The governing equation of motion for free vibration of the fluid-conveying pipe is derived by applying the Timoshenko elastic theory.

The components of stress and strain are represented using the displacements as given in equation 1.

$$\sigma_{xx} = -EZ \frac{\partial \phi}{\partial x}; \quad \varepsilon_{xx} = -Z \frac{\partial \phi}{\partial x} \quad (2)$$

$$\sigma_{zx} = KG \left( \frac{\partial w}{\partial x} - \phi \right); \quad \varepsilon_{zx} = -\phi + \frac{\partial w}{\partial x} \quad (3)$$

$$\varepsilon_{yz} = \varepsilon_{xy} = \varepsilon_{yy} = \varepsilon_{zz} = \sigma_{yy} = \sigma_{zz} = \sigma_{xy} = \sigma_{yz} = 0 \quad (4)$$

The strain energy of the system is expressed as

$$\pi_1 = \frac{1}{2} \iiint_V (\sigma_{xx} \varepsilon_{xx} + \sigma_{yy} \varepsilon_{yy} + \sigma_{zz} \varepsilon_{zz} + \sigma_{xy} \varepsilon_{xy} + \sigma_{yz} \varepsilon_{yz} + \sigma_{zx} \varepsilon_{zx}) dv \quad (5)$$

$$\pi_1 = \frac{1}{2} \int_0^L \iint_A (\sigma_{xx} \varepsilon_{xx} + \sigma_{zx} \varepsilon_{zx}) dA. dx$$

On the substitution of equations 2, 3 and 4

$$\pi_1 = \frac{1}{2} \int_0^L \iint_A \left[ EZ^2 \left( \frac{\partial \phi}{\partial x} \right)^2 + KG \left( \frac{\partial w}{\partial x} - \phi \right)^2 \right] dA. dx$$

$$\pi_1 = \frac{1}{2} \int_0^L \iint_A \left[ EAZ^2 \left( \frac{\partial \phi}{\partial x} \right)^2 + KAG \left( \frac{\partial w}{\partial x} - \phi \right)^2 \right] dA. dx \quad (6)$$

Equation 6 is written as  $AZ^2 = I$ , where I is the moment of inertia of bellow

$$\pi_1 = \frac{1}{2} \int_0^L \left[ EI \left( \frac{\partial \phi}{\partial x} \right)^2 + KAG \left( \frac{\partial w}{\partial x} - \phi \right)^2 \right] dx \quad (7)$$

Strain energy due to Pressure,

$$\pi_2 = \frac{1}{2} \int_0^L \left[ P \pi R_m^2 \left( \frac{\partial w}{\partial x} \right)^2 \right] dx \quad (8)$$

The Stain energy due to temperature

On addition of equations 6, 7, 8 and 9 the total strain energy equation

$$\pi = \pi_1 + \pi_2$$

$$\pi = \frac{1}{2} \int_0^L \left[ EI \left( \frac{\partial \phi}{\partial x} \right)^2 + KAG \left( \frac{\partial w}{\partial x} - \phi \right)^2 \right] dx + \frac{1}{2} \int_0^L \left[ P \pi R_m^2 \right] \left( \frac{\partial w}{\partial x} \right)^2 dx \quad (9)$$

The Kinetic energy is

$$T = \frac{1}{2} \int_0^L \left[ (m_p + m_f) \left( \frac{\partial u}{\partial t} \right)^2 - 2m_f U \sin \theta \frac{\partial w}{\partial t} \right] dx + \frac{\rho_p l}{2} \int_0^L \left( \frac{\partial \phi}{\partial t} \right)^2 dx + \frac{1}{2} \int_0^L \left[ (m_p + m_f) \left( \frac{\partial w}{\partial t} \right)^2 + 2m_f U \cos \theta \frac{\partial w}{\partial t} \right] dx + \frac{m_f}{2} \int_0^L U^2 dx + \frac{\rho_f l}{2} \int_0^L \left( \frac{\partial^2 \phi}{\partial x \partial t} \right)^2 dx \quad (10)$$

Now eliminating non-linear terms and  $\sin \theta = \frac{\partial w}{\partial x}$

$$T = \frac{1}{2} \int_0^L \left[ -2m_f U \frac{\partial w}{\partial t} \frac{\partial w}{\partial t} \right] dx + \frac{\rho_p l}{2} \int_0^L \left( \frac{\partial \phi}{\partial t} \right)^2 dx + \frac{1}{2} \int_0^L \left[ (m_p + m_f) \left( \frac{\partial w}{\partial t} \right)^2 \right] dx + \frac{\rho_f l}{2} \int_0^L \left( \frac{\partial^2 \phi}{\partial x \partial t} \right)^2 dx \quad (11)$$

Applying the virtual work principle, we have

$$VW = \int_0^L f w dx - \int_0^L m_f U^2 \left( \frac{\partial w}{\partial x} \right) \cos \theta dx - \int_0^L m_f U^2 \left( \frac{\partial w}{\partial x} \right) \sin \theta dx \quad (12)$$

And elimination of non-linear terms and  $\cos \theta$  and  $\sin \theta$

$$VW = - \int_0^L m_f U^2 \left( \frac{\partial w}{\partial t} \right)^2 dx \quad (13)$$

Substituting in Hamilton Principle gives

$$\delta \int_{t_1}^{t_2} [\pi - T - VW] dt = 0 \quad (14)$$

$$\int_{t_1}^{t_2} [\delta \pi - \delta T - \delta(VW)] dt = 0 \quad (15)$$

Consider

$$\int_{t_1}^{t_2} \delta \pi dt = \int_{t_1}^{t_2} \int_0^L \left[ EI \left( \frac{\partial \phi}{\partial x} \right) \delta \left( \frac{\partial \phi}{\partial x} \right) \right] dx dt + \int_{t_1}^{t_2} \int_0^L KAG \left( \frac{\partial w}{\partial x} - \phi \right) \delta \left( \frac{\partial w}{\partial x} - \phi \right) dx dt$$

$$+ \int_{t_1}^{t_2} \int_0^L \left[ P \pi R_m^2 \right] \left( \frac{\partial w}{\partial x} \right) \delta \left( \frac{\partial w}{\partial x} \right) dt$$

$$\int_{t_1}^{t_2} \delta \pi dt = \int_{t_1}^{t_2} \left[ \left\{ EI \left( \frac{\partial \phi}{\partial x} \right) \delta \phi \right\}_0^l - \int_0^l EI \frac{\partial^2 \phi}{\partial x^2} \delta \phi dx \right] dt + \int_{t_1}^{t_2} \left[ \left\{ kAG \left( \frac{\partial w}{\partial x} - \phi \right) \delta \phi \right\}_0^l - \int_0^l kAG \left( \frac{\partial^2 w}{\partial x^2} - \frac{\partial \phi}{\partial x} \right) \delta w dx \right] dt + \int_{t_1}^{t_2} \int_0^l kAG \left( \frac{\partial w}{\partial x} - \phi \right) \delta \phi dx dt + \int_{t_1}^{t_2} \left[ \left\{ [P\pi R_m^2] \left( \frac{\partial w}{\partial x} \right) \delta w \right\}_0^l - \int_0^l [P\pi R_m^2] \frac{\partial^2 w}{\partial x^2} \delta w dx \right] dt \quad (16)$$

The Kinetic Energy term is

$$\int_{t_1}^{t_2} \delta T dt = - \int_{t_1}^{t_2} \left[ \int_0^l 2m_f U \frac{\partial w}{\partial t} \delta \frac{\partial w}{\partial t} dx \right] dt + \rho_p I \int_{t_1}^{t_2} \left[ \int_0^l \frac{\partial \phi}{\partial t} \delta \frac{\partial \phi}{\partial t} dx \right] dt + (m_p + m_f) \int_{t_1}^{t_2} \left[ \int_0^l \frac{\partial w}{\partial t} \delta \frac{\partial w}{\partial t} dx \right] dt + \rho_f I \int_{t_1}^{t_2} \left[ \int_0^l \left( \frac{\partial^2 \phi}{\partial x \partial t} \right) \delta \left( \frac{\partial^2 \phi}{\partial x \partial t} \right) dx \right] dt$$

$$\int_{t_1}^{t_2} \delta T dt = - \int_{t_1}^{t_2} \left[ \left\{ 2m_f U \frac{\partial w}{\partial t} \delta w \right\}_0^l - \int_0^l 2m_f \frac{\partial^2 w}{\partial x \partial t} \delta w dx \right] dt + \rho_p I \int_{t_1}^{t_2} \left[ \left\{ \frac{\partial \phi}{\partial t} \delta \phi \right\}_0^l - \int_0^l \frac{\partial^2 \phi}{\partial t^2} \delta \phi dx \right] dt + (m_p + m_f) \int_{t_1}^{t_2} \left[ \left\{ \frac{\partial w}{\partial t} \delta w \right\}_0^l - \int_0^l \frac{\partial^2 w}{\partial t^2} \delta w dx \right] dt + \rho_p I \int_{t_1}^{t_2} \left[ \left\{ \left( \frac{\partial^2 \phi}{\partial x \partial t} \right) \frac{\partial \phi}{\partial t} \delta \phi \right\}_0^l - \int_0^l \frac{\partial^3 \phi}{\partial x^2 \partial t} \delta \phi dx \right] dt \quad (17)$$

Consider the virtual work

$$\int_{t_1}^{t_2} \delta (VW) dt = - \int_{t_1}^{t_2} \left[ \int_0^l m_f U^2 \left( \frac{\partial w}{\partial x} \right) \delta \left( \frac{\partial w}{\partial x} \right) dx \right] dt$$

$$= - \int_{t_1}^{t_2} \left[ \left\{ m_f U^2 \frac{\partial w}{\partial x} \delta w \right\}_0^l - \int_0^l m_f U^2 \frac{\partial^2 w}{\partial x^2} \delta w dx \right] dt \quad (18)$$

On substitution of 17, 18, and 19 in 16 gives

$$\int_{t_1}^{t_2} \left[ \left\{ EI \left( \frac{\partial \phi}{\partial x} \right) \delta \phi \right\}_0^l - \int_0^l EI \frac{\partial^2 \phi}{\partial x^2} \delta \phi dx \right] dt + \int_{t_1}^{t_2} \left[ \left\{ kAG \left( \frac{\partial w}{\partial x} - \phi \right) \delta \phi \right\}_0^l - \int_0^l kAG \left( \frac{\partial^2 w}{\partial x^2} - \frac{\partial \phi}{\partial x} \right) \delta w dx \right] dt + \int_{t_1}^{t_2} \int_0^l kAG \left( \frac{\partial w}{\partial x} - \phi \right) \delta \phi dx dt + \int_{t_1}^{t_2} \left[ \left\{ [P\pi R_m^2] \left( \frac{\partial w}{\partial x} \right) \delta w \right\}_0^l - \int_0^l [P\pi R_m^2] \frac{\partial^2 w}{\partial x^2} \delta w dx \right] dt + \int_{t_1}^{t_2} \left[ \left\{ 2m_f U \frac{\partial w}{\partial t} \delta w \right\}_0^l - \int_0^l 2m_f \frac{\partial^2 w}{\partial x \partial t} \delta w dx \right] dt + \rho_p I \int_{t_1}^{t_2} \left[ \left\{ \frac{\partial \phi}{\partial t} \delta \phi \right\}_0^l - \int_0^l \frac{\partial^2 \phi}{\partial t^2} \delta \phi dx \right] dt + (m_p + m_f) \int_{t_1}^{t_2} \left[ \left\{ \frac{\partial w}{\partial t} \delta w \right\}_0^l - \int_0^l \frac{\partial^2 w}{\partial t^2} \delta w dx \right] dt + \rho_p I \int_{t_1}^{t_2} \left[ \left\{ \left( \frac{\partial^2 \phi}{\partial x \partial t} \right) \frac{\partial \phi}{\partial t} \delta \phi \right\}_0^l - \int_0^l \frac{\partial^3 \phi}{\partial x^2 \partial t} \delta \phi dx \right] dt + \int_{t_1}^{t_2} \left[ \left\{ m_f U^2 \frac{\partial w}{\partial x} \delta w \right\}_0^l - \int_0^l m_f U^2 \frac{\partial^2 w}{\partial x^2} \delta w dx \right] dt = 0 \quad (19)$$

Now considering terms  $\delta w dx dt$

$$kAG \left( \frac{\partial^2 w}{\partial x^2} - \frac{\partial \phi}{\partial x} \right) - [P\pi R_m^2] \frac{\partial^2 w}{\partial x^2} - 2m_f \frac{\partial^2 w}{\partial x \partial t} - (m_{tot}) \frac{\partial^2 w}{\partial t^2} + m_f U^2 \frac{\partial^2 w}{\partial x^2} = 0 \quad (20)$$

$$-(kAG + P\pi R_m^2 + m_f U^2) \frac{\partial^2 w}{\partial x^2} + kAG \frac{\partial \phi}{\partial x} - 2m_f \frac{\partial^2 w}{\partial x \partial t} - (m_{tot}) \frac{\partial^2 w}{\partial t^2} = 0$$

$$kAG \frac{\partial \phi}{\partial x} = (kAG + P\pi R_m^2 + m_f U^2) \frac{\partial^2 w}{\partial x^2} + 2m_f \frac{\partial^2 w}{\partial x \partial t} + (m_{tot}) \frac{\partial^2 w}{\partial t^2}$$

Divide with kAG

$$\frac{\partial \phi}{\partial x} = \left( 1 + \frac{P\pi R_m^2 + m_f U^2}{kAG} \right) \frac{\partial^2 w}{\partial x^2} + \frac{2m_f}{kAG} \frac{\partial^2 w}{\partial x \partial t} + \frac{m_{tot}}{kAG} \frac{\partial^2 w}{\partial t^2} \quad (21)$$

Now consider term  $\delta \phi dx dt$

$$EI \frac{\partial^2 \phi}{\partial x^2} - kAG \frac{\partial w}{\partial x} + kAG \phi + \rho_p I \frac{\partial^2 \phi}{\partial t^2} - \rho_p I \frac{\partial^3 \phi}{\partial x^2 \partial t} = 0 \quad (22)$$

The equation. 23, on differentiation with respect to dx

$$EI \frac{\partial^2}{\partial x^2} \left( \frac{\partial \phi}{\partial x} \right) - kAG \frac{\partial^2 w}{\partial x^2} + kAG \left( \frac{\partial \phi}{\partial x} \right) + \rho_p I \frac{\partial^2}{\partial t^2} \left( \frac{\partial \phi}{\partial x} \right) - \rho_p I \frac{\partial^3}{\partial x^2 \partial t} \left( \frac{\partial \phi}{\partial x} \right) = 0 \quad (23)$$

On substitution of  $\frac{\partial \phi}{\partial x}$  in equation. 24, we get

$$EI \left( 1 + \frac{P\pi R_m^2 + m_f U^2}{kAG} \right) \frac{\partial^4 w}{\partial x^4} - EI \frac{m_{tot}}{kAG} \frac{\partial^4 w}{\partial x^2 \partial t^2} - kAG \frac{\partial^2 w}{\partial x^2} + kAG \frac{\partial^2 w}{\partial x^2} + (P\pi R_m^2 + m_f U^2) \frac{\partial^2 w}{\partial x^2} - 2m_f U \frac{\partial^2 w}{\partial x \partial t} + (m_p + m_f) \frac{\partial^2 w}{\partial t^2} - \rho_p I \frac{\partial^4 w}{\partial x^2 \partial t^2} - \rho_p I \frac{m_{tot}}{kAG} \frac{\partial^4 w}{\partial t^4} = 0 \quad (24)$$

Eliminating non-linear terms

$$EI \frac{\partial^4 w}{\partial x^4} - (\rho_p I + EI \frac{m_{tot}}{kAG}) \frac{\partial^4 w}{\partial x^2 \partial t^2} + (m_p + m_f) \frac{\partial^2 w}{\partial t^2} + (P\pi R_m^2 + m_f U^2) \frac{\partial^2 w}{\partial x^2} - 2m_f U \frac{\partial^2 w}{\partial x \partial t} - \rho_p I \frac{m_{tot}}{kAG} \frac{\partial^4 w}{\partial t^4} = 0 \quad (25)$$

Now, boundary conditions with respect to  $\delta w$

$$kAG \left( \frac{\partial w}{\partial x} - \phi \right) - [P\pi R_m^2 + m_f U^2] \frac{\partial w}{\partial x} + 2m_f U \frac{\partial w}{\partial t} = 0 \quad (26)$$

$$kAG \left( \frac{\partial w}{\partial x} \right) - kAG \phi - [P\pi R_m^2 + m_f U^2] \frac{\partial w}{\partial x} + 2m_f U \frac{\partial w}{\partial t} = 0 \quad (27)$$

In equation. 26 the rotary inertia and shear is calculated as 5.2508e-11 and 0.7615e-3 respectively. As shear component is very negligible and it has been neglected.

The equation.25 can be rewritten as-

$$EI \frac{\partial^4 w}{\partial x^4} + (P\pi R_m^2 + m_f U^2) \frac{\partial^2 w}{\partial x^2} - J \frac{\partial^4 w}{\partial x^2 \partial t^2} + (m_p + m_f) \frac{\partial^2 w}{\partial t^2} = 0 \quad (28)$$

Where EI, P, T, E, J, w, x, m<sub>p</sub>, m<sub>f</sub> are bending stiffness, pressure, temperature, modulus of elasticity, total mass moment of inertia per unit length, deflection, axial coordinate, the mass of bellow and the mass of the fluid

The dimensionless parameters are defined as

$$x = \frac{x}{L}, y = \frac{w}{L}, m = \frac{m_f}{m_p + m_f}, \eta = \frac{PAL^2}{EI}, \zeta = \frac{m_f U^2 L}{EI}, \phi = \frac{J\omega^2 L^2}{EI} \text{ and } \lambda = \frac{m_{tot}\omega^2}{EI} \quad (29)$$

Using the Equation. 29 and 30, the governing differential equation of motion can be reduced to the following dimensionless form

$$\frac{\partial^4 w}{\partial x^4} + (\eta + \zeta) \frac{\partial^2 w}{\partial x^2} + \phi \frac{\partial^2 w}{\partial x^2} - \lambda^4 w = 0 \quad (30)$$

Using the technique of separation of variables, the lateral deflection of the bellows axis 'w' can be expressed as

$$w(x, t) = X(x).T(t) \text{ and } T(t) = A e^{i\omega t} \quad (31)$$

Differentiating the above equation (31) and substituting into the differential equation. 30 we get,

$$\frac{\partial^4 X}{\partial x^4} + (\eta + \zeta + \phi) \times \frac{\partial^2 X}{\partial x^2} - \omega^2 \frac{m_{tot}}{EI} X = 0 \quad (32)$$

$$\text{If } c = \sqrt{(\eta + \zeta + \phi)}, \quad (33)$$

Then equation. 32 can be written as

$$\frac{d^4 X}{dx^4} + 2c^2 \frac{d^2 X}{dx^2} - \lambda^4 X = 0 \quad (34)$$

Assuming a general solution of equation. 34 is given by

$$X(x) = A \sinh \alpha x + B \cosh \alpha x + C \sin \beta x + D \cos \beta x \quad (35)$$

Where A, B, C, D are arbitrary constants respectively. The first derivatives of the equation. 35 are as follows

$$\frac{dX(x)}{dx} = A.\alpha \cosh \alpha x + B. \sinh \alpha x + C.\beta \cos \beta x + D. \beta \sin \beta x \quad (36)$$

Let the roots of the equation. 36 be  $\alpha$  &  $\beta$

$$\alpha = \sqrt{-c^2 + \sqrt{c^4 + \lambda^4}} \quad (37)$$

$$\beta = \sqrt{c^2 + \sqrt{c^4 + \lambda^4}} \quad (38)$$

And

$$\lambda = \sqrt[4]{\frac{m_{tot} \cdot \omega^2}{EI}} \quad (39)$$

The fixed-fixed boundary conditions are

$$w(0, t) = w(l, t) = \frac{\partial w(0, t)}{\partial x} = \frac{\partial w(l, t)}{\partial x} = 0 \quad (40)$$

The boundary conditions given by the Equation. 40) corresponding to conditions of zero displacement and zero slope at  $x = 0$  and  $x = L$  respectively.

The solution of the differential equation. 34 can be expressed as

$$W(X) = C e^{i\omega t} \quad (41)$$

Where  $\omega$  is circular frequency and C is arbitrary constant

On substitution of Equation. 41 in Equation. 37 the following equation is obtained

$$A = 0 \quad (42)$$

$$\alpha B + \beta D = 0 \quad (43)$$

$$A \cosh \alpha l + B \sinh \alpha l + C \cos \beta l + D \sin \beta l = 0 \quad (44)$$

$$A \alpha \sinh \alpha l + B \alpha \cosh \alpha l - C \beta \sin \beta l + D \beta \cos \beta l = 0 \quad (45)$$

Determinate for the above four equations 43, 44, 45 and 46

$$\begin{vmatrix} 1 & 0 & 1 & 0 \\ 0 & \alpha & 0 & \beta \\ \cosh \alpha l & \sinh \alpha l & \cos \beta l & \sin \beta l \\ \alpha \sinh \alpha l & \alpha \cosh \alpha l & -\beta \sin \beta l & \beta \cos \beta l \end{vmatrix} = 0 \quad (46)$$

$$2\alpha\beta[1 - \cosh(\alpha l) \cdot \cos(\beta l)] + [(\alpha^2 - \beta^2)] \sinh(\alpha l) \cdot \sin(\beta l) = 0 \quad (47)$$

Equation. 47 is closed from the transcendental equation for finding the natural frequencies of transverse vibration of single bellow expansion joint. Using the Muller's bisection method, the characteristic equation. 47 is solved for four modes of vibration.

### III. RESULT AND DISCUSSION

In this paper, the free vibration equation of the fluid conveying PTFE bellows expansion joint is derived by using Timoshenko elastic theory. The results are obtained by analyzing the effect of pressure and combined effect of pressure and temperature of the fluid (water) on the frequencies at different modes.



**a. Frequency with change of inlet pressure**

Table 1 presents the influence of pressure variation on the four modes of vibration. The frequencies are obtained in non-dimensional form. Table 1 and Fig 4 represent the change of frequency with respect to inlet pressure. Bellows become unstable at critical pressure when the non-dimensional frequency becomes zero. It is found that the critical pressure of bellows approaches 13 for first mode, 26 for second mode, 49 for third mode and 73 for fourth respectively. It is found that the bellows are instable

Table 1: Fundamental natural frequencies for varying inlet pressure

| S No | Non-dimensional Pressure ( $\eta$ ) | Non- dimensional frequency |          |          |          |
|------|-------------------------------------|----------------------------|----------|----------|----------|
|      |                                     | Mode-1                     | Mode-2   | Mode-3   | Mode-4   |
| 1    | 0.0                                 | 3.06E+01                   | 8.45E+01 | 1.66E+02 | 2.74E+02 |
| 2    | 5.0                                 | 2.34E+01                   | 7.54E+01 | 1.56E+02 | 2.64E+02 |
| 3    | 10.0                                | 1.21E+01                   | 6.50E+01 | 1.46E+02 | 2.53E+02 |
| 4    | 12.6                                | 0.00E+00                   | 5.77E+01 | 1.39E+02 | 2.47E+02 |
| 5    | 14.0                                |                            | 5.51E+01 | 1.37E+02 | 2.45E+02 |
| 6    | 15.0                                |                            | 5.24E+01 | 1.35E+02 | 2.42E+02 |
| 7    | 20.0                                |                            | 3.53E+01 | 1.22E+02 | 2.31E+02 |
| 8    | 25.0                                |                            | 5.90E+00 | 1.09E+02 | 2.19E+02 |
| 9    | 26.0                                |                            | 0.00E+00 | 1.06E+02 | 2.17E+02 |
| 10   | 30.0                                |                            |          | 9.40E+01 | 2.06E+02 |
| 11   | 35.0                                |                            |          | 7.66E+01 | 1.93E+02 |
| 12   | 40.0                                |                            |          | 5.57E+01 | 1.79E+02 |
| 13   | 45.0                                |                            |          | 2.80E+01 | 1.63E+02 |
| 14   | 49.0                                |                            |          | 0.00E+00 | 1.50E+02 |
| 15   | 73.0                                |                            |          |          | 0.00E+00 |

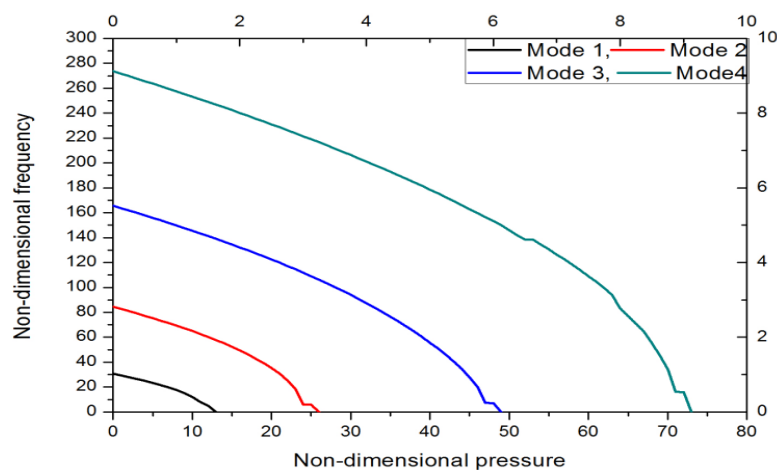


Figure 4: Frequency for combined effect of pressure and temperature

**b. Frequency with change of inlet velocity**

Table 2 presents the influence of velocity variation on the four modes of vibrations. The frequencies are obtained in non-dimensional form. Table 2 and Fig 5 represent the change of frequency with respect to inlet velocity. Bellows become unstable at critical velocity when the non-dimensional frequency becomes zero. It is found that critical velocity of bellows approaches 15 for first mode, 22 for second mode, 30 for third mode and 37 for fourth respectively. It is found that the bellows are instable

Table 2: Fundamental natural frequencies for varying inlet pressure

| S.No | Non-dimensional Velocity ( $\zeta$ ) | Non- dimensional frequency |          |          |          |
|------|--------------------------------------|----------------------------|----------|----------|----------|
|      |                                      | Mode 1                     | Mode 2   | Mode 3   | Mode 4   |
| 1    | 0.0                                  | 3.06E+01                   | 8.45E+01 | 1.65E+02 | 2.74E+02 |
| 2    | 1.0                                  | 3.06E+01                   | 8.44E+01 | 1.66E+02 | 2.74E+02 |
| 3    | 5.0                                  | 2.89E+01                   | 8.48E+01 | 1.63E+02 | 2.71E+02 |
| 4    | 10.0                                 | 2.29E+01                   | 7.48E+01 | 1.55E+02 | 2.63E+02 |
| 5    | 14.0                                 | 1.07E+01                   | 6.41E+01 | 1.45E+02 | 2.52E+02 |
| 6    | 14.8                                 | 0.00E+00                   | 6.04E+01 | 1.41E+02 | 2.49E+02 |
| 7    | 20.0                                 |                            | 2.96E+01 | 1.19E+02 | 2.28E+02 |
| 8    | 21.0                                 |                            | 1.48E+01 | 1.14E+02 | 2.23E+02 |
| 9    | 22.0                                 |                            | 0.00E+00 | 1.07E+02 | 2.19E+02 |
| 10   | 25.0                                 |                            |          | 8.34E+01 | 1.98E+02 |
| 11   | 29.0                                 |                            |          | 3.06E+01 | 1.66E+02 |
| 12   | 30.0                                 |                            |          | 0.00E+00 | 1.54E+02 |
| 13   | 36.0                                 |                            |          |          | 4.82E+01 |
| 14   | 37.0                                 |                            |          |          | 0.00E+00 |

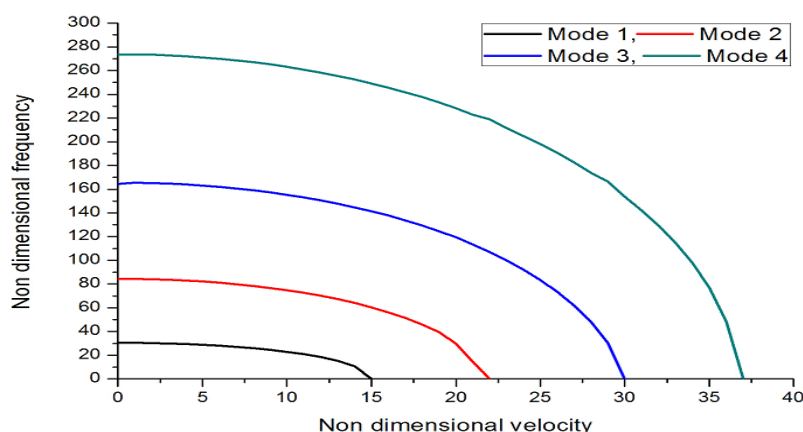


Figure 5: non- dimensional frequency for effect of non-dimensional velocity

Fig 6 represents the comparison of Non- dimensional pressure and non-dimensional velocity on the non-dimensional frequency. The critical pressure and critical velocity of the bellows found as non-dimensional pressure and non-dimensional velocity at 15.

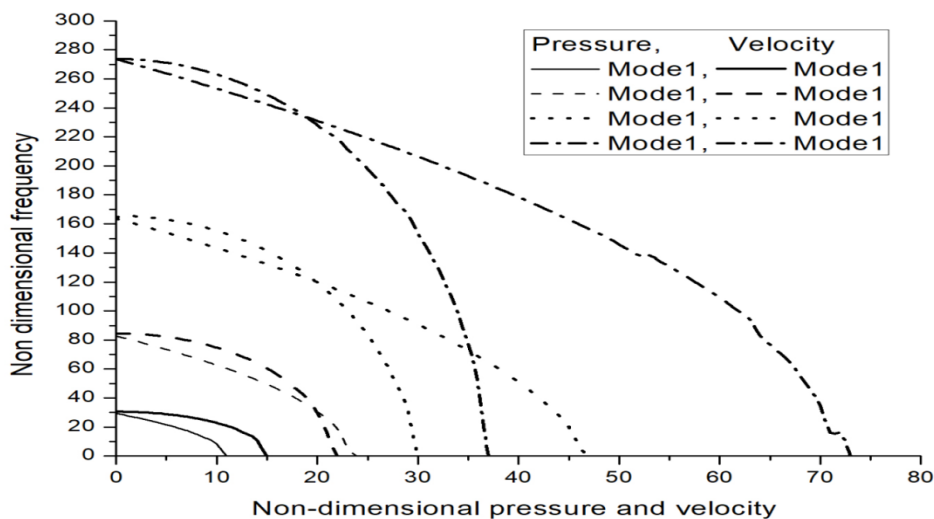


Figure 6: non- dimensional frequency for effect of non-dimensional velocity and pressure



### c. Comparison of theoretical and experimental results

The properties and the geometry of the PTFE bellows expansion joint consider as that the density of Polytetrafluoroethylene bellows expansion joint (PTFEBEJ) is  $2300 \text{ kg/m}^3$ ; bending rigidity  $4.4692 \text{ Nm}$ ; the mass of the fluid in bellow per unit length of PTFEBEJ is  $2.859 \text{ kg}$  and the mass per unit length of the PTFEBEJ is  $3.7718 \text{ kg}$ . Geometric and material parameters: diameter of bellow,  $D_m = 80.0 \text{ mm}$ ; thickness of bellow,  $t_p = 2 \text{ mm}$ ; Pitch of bellow,  $q = 5 \text{ mm}$ ; length of bellow,  $L = 32.1 \text{ mm}$ ; convolution height of bellow,  $h = 5.71 \text{ mm}$ ; Young's modulus of the bellow,  $E_{\text{PTFE}} = 1.5 \times 10^9 \text{ N/m}^2$ ; Root and crown radius  $R_1 = R_2 = 12.5 \text{ mm}$ .

The experimental setup in Fig 7 consists of  $80 \text{ mm}$  outer diameter PTFE bellow which is fixed at both ends and connected with pipes for fluid flow. A globe valve is used to regulate inlet pressure and pressure gauges and thermocouples are mounted to measure the inlet and outlet pressures and temperatures. A piezoelectric transducer (Accelerometer) is installed on the bellow at different positions to obtain frequencies in terms of velocity and displacement. The Vibration analyzer, signal records the waveform in Fig 8. Properties of PTFE bellow for comparing theoretical results are given below. The fig 8 represents the wave foe experimental result in mode 2 at non- dimensional velocity  $5.0$

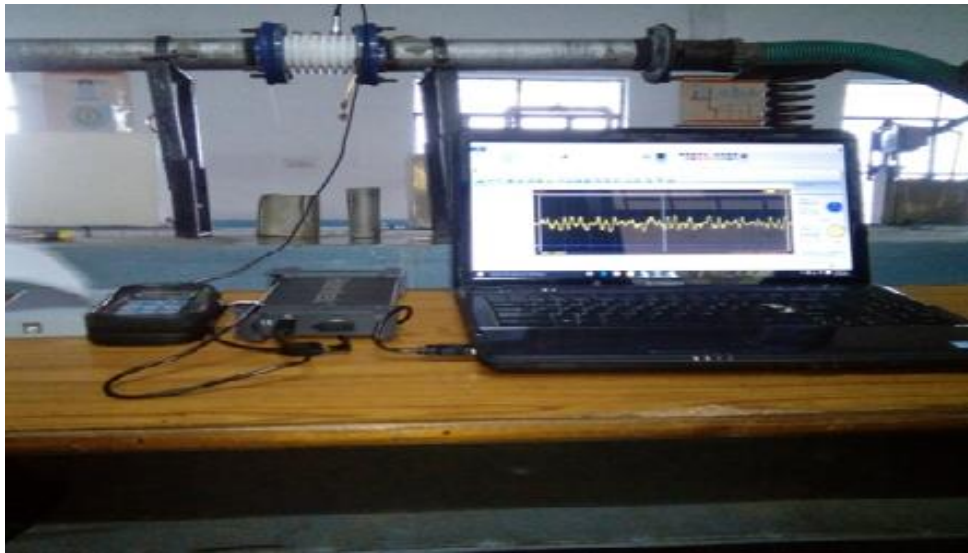


Figure 7: Experimental setup of PTFE bellows

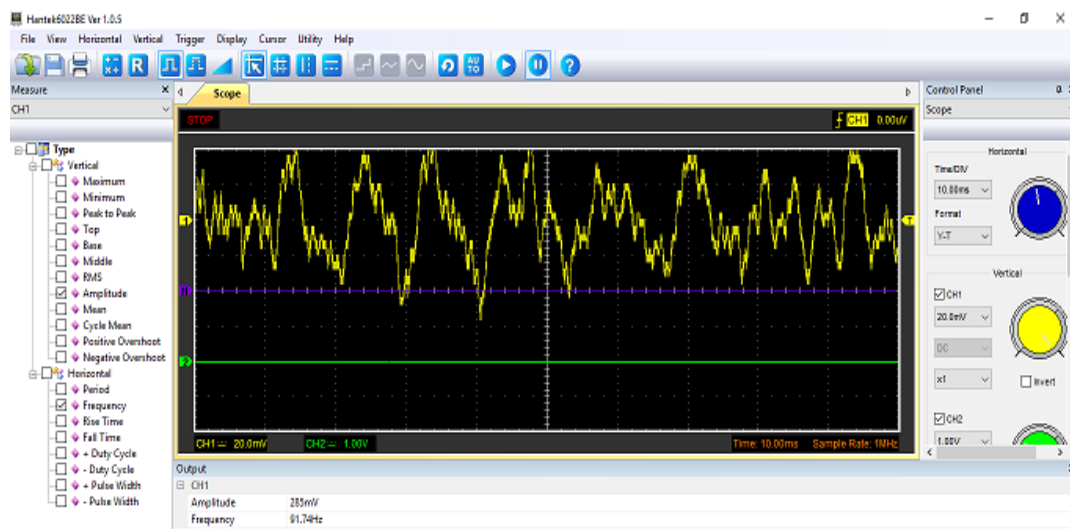


Figure 8: Experimental result for Mode 2 at Non- dimensional velocity  $5.0$

Table 3 and fig 9 represents a comparison and validation of results found by theory and experiments. It is observed that at  $\eta = 5.0$  the frequency at Mode 1 is obtained as  $23.43$  by exact solution and  $25.12$  from experiment with percentage error of  $3\%$ .

Table 3: Comparison of theoretical and experimental results

| S.No | Non-dimensional Pressure ( $\eta$ ) | Non- dimensional Frequency at different modes |             |              |                         |
|------|-------------------------------------|---|-------------|--------------|-------------------------|
|      |                                     | Modes   | Theoretical | Experimental | Percentage of error (%) |
| 1    | 5.0                                 | 1   | 23.43       | 27.12        | 3                       |
|      |                                     | 2   | 75.49       | 81.23        | 7                       |
|      |                                     | 3   | 156.58      | 165.76       | 5                       |
|      |                                     | 4   | 264.65      | 278.29       | 4                       |

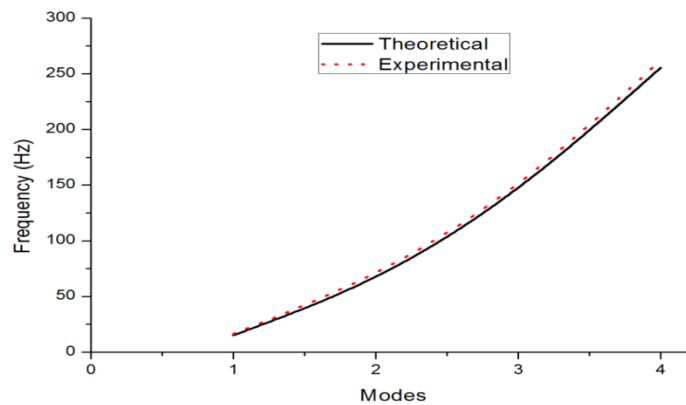


Figure 9: Comparison of theoretical and experimental results in non-dimensional pressure 5.0

Table 4 and fig 10 represents a comparison and validation of results found by theory and experiments. It is observed that at  $\zeta = 5.0$  the frequency at Mode 1 is obtained as 28.54 by exact solution and 30.83 from experiment with percentage error of 4%.

Table 4: Comparison of theoretical and experimental results

| S.No | Non-dimensional Velocity ( $\zeta$ ) | Non- dimensional Frequency at different modes |             |              |                         |
|------|--------------------------------------|---|-------------|--------------|-------------------------|
|      |                                      | Modes   | Theoretical | Experimental | Percentage of error (%) |
| 1    | 5.0                                  | 1   | 28.54       | 30.83        | 4                       |
|      |                                      | 2   | 84.85       | 91.7         | 7                       |
|      |                                      | 3   | 163.85      | 172.19       | 4                       |
|      |                                      | 4   | 271.63      | 286.57       | 5                       |

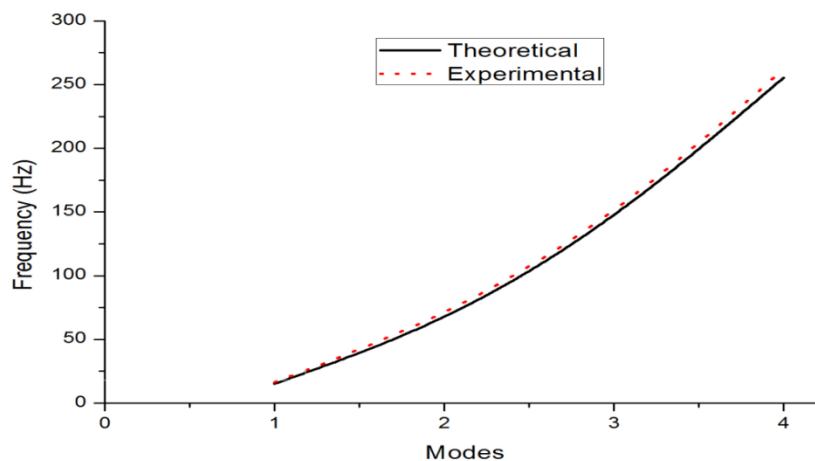


Figure 10: Comparison of theoretical and experimental results under change of non-dimensional velocity 5.0.

#### IV. CONCLUSION

The transverse vibration analysis of a fluid conveying PTFE bellows expansion joint under the effect of pressure and velocity change with fixed ends was studied. Based on the analysis it was observed that the

influence of pressure on the fundamental frequency of the fixed PTFE bellows expansion joint is significant and recorded as non-dimensional critical pressure is 12.6 and the critical velocity recorded as 14.8. Results show that the pressures and velocity under effect on the frequency becomes significant with increase in pressure and velocity parameters individually thereon leads to a decrease in the frequency. The experimental results have confirmed that the transcendental frequency equation derived is exact, within the engineering accuracy of less than 10%. It was studied that any change in each pressure and velocity individually will significantly affect the performance of the bellow, and might lead to a failure even before the design conditions are attained.

## V. ACKNOWLEDGMENT

The authors wish to thank the Sai Spurthi Institute of Technology-Sathupally, Telangana, India and CSIR-Indian Institute of Chemical Technology-Hyderabad in India for providing the experimental and computational support for the study.

## REFERENCES

- [1]. Jakubauskas VF, Weaver DS. Axial Vibrations of Fluid-Filled Bellows Expansion Joints. *J Press Vessel Technol* 1996;118(4):484–90.
- [2]. Jakubauskas VF, Weaver DS. Transverse Natural Frequencies and Flow-Induced Vibrations of Double Bellows Expansion Joints. *J Fluids Struct* 1999;13:461–79. doi:10.1006/jfls.1999.0215.
- [3]. Jakubauskas VF, Weaver DS. Transverse Vibrations of Bellows Expansion Joints. Part I: Fluid Added Mass. *J Fluids Struct* 1998;12:445–56. doi:10.1006/jfls.1997.0151.
- [4]. Jakubauskas VF, Weaver DS. Transverse Vibrations of Bellows Expansion Joints. Part II: Beam Model Development and Experimental Verification. *J Fluids Struct* 1998;12:457–73. doi:10.1006/jfls.1997.0152.
- [5]. Jakubauskas VF. Added Fluid Mass for Bellows Expansion Joints in Axial Vibrations. *J Press Vessel Technol* 1999;121:216. doi:10.1115/1.2883689.
- [6]. Radhakrishna M, Kameswara Rao C. Axial vibrations of U-shaped bellows with elastically restrained end conditions. *Thin-Walled Struct* 2004;42:415–26. doi:10.1016/S0263-8231(03)00130-7.
- [7]. Watanabe M, Kobayashi N, Wada Y. Dynamic Stability of Flexible Bellows Subjected to Periodic Internal Fluid Pressure Excitation. *J Press Vessel Technol* 2004;126:188. doi:10.1115/1.1687380.
- [8]. Faraji G, Mashhadi MM, Norouzfard V. Evaluation of effective parameters in metal bellows forming process. *J Mater Process Technol* 2009;209:3431–7. doi:10.1016/j.jmatprotec.2008.07.057.
- [9]. Price DM, Jarratt M. Thermal conductivity of PTFE and PTFE composites. *Thermochim Acta* 2002;392–393:231–6. doi:10.1016/S0040-6031(02)00105-3.
- [10]. Rae PJ, Dattelbaum DM. The properties of poly(tetrafluoroethylene) (PTFE) in compression. *Polymer (Guildf)* 2004;45:7615–25. doi:10.1016/j.polymer.2004.08.064.
- [11]. Wilson JF. Mechanics of bellows: A critical survey. *Int J Mech Sci* 1984;26:593–605. doi:10.1016/0020-7403(84)90013-4.
- [12]. Wilson JF. Mechanics of fluid-activated, clustered satellite bellows. *Int J Solids Struct* 2008;45:4173–83. doi:10.1016/j.ijsolstr.2008.02.027.
- [13]. Becht C. Fatigue of bellows, a new design approach. *International Journal of Pressure Vessels and Piping*, 77(13), 843–850. [https://doi.org/10.1016/S0308-0161\(00\)00078-8](https://doi.org/10.1016/S0308-0161(00)00078-8). *Int J Press Vessel Pip* 2000;77:843–50. doi:10.1016/S0308-0161(00)00078-8.
- [14]. Tingxin L, Xiaoping L, Tianxiang L, Xigang H, Xinfeng L. Experimental research of toroid-shaped bellows behavior. *Int J Press Vessel Pip* 1995;63:141–6. doi:10.1016/0308-0161(94)00031-D.
- [15]. Shaikh H, George G, Singh Khatak H. Failure analysis of an AM 350 steel bellows. *Eng Fail Anal* 2001;8:571–6. doi:10.1016/S1350-6307(00)00026-1.
- [16]. Nishiguchi I, Kashiwabara S. On the pressure buckling of rectangular bellows for fusion reactors. *Fusion Eng Des* 1998;41:323–9. doi:10.1016/S0920-3796(98)00255-5.
- [17]. Broman GI, Jönsson AP, Hermann MP. Determining dynamic characteristics of bellows by manipulated beam finite elements of commercial software. *Int J Press Vessel Pip* 2000;77:445–53. doi:10.1016/S0308-0161(00)00046-6.
- [18]. Li TX, Guo BL, Li TX. Natural frequencies of U-shaped bellows. *Int J Press Vessel Pip* 1990;42:61–74. doi:10.1016/0308-0161(90)90055-M.

Sujan Rao. Nakkanti "Study on the Influence of Fluid Parameters on Transverse Vibrations of Polytetrafluoroethylene Bellows Expansion Joint." *IOSR Journal of Engineering (IOSRJEN)*, vol. 08, no. 6, 2018, pp. 58-68.